Published in final edited form as:

Circulation. 2018 November 20; 138(21): 2395–2412. doi:10.1161/CIRCULATIONAHA.118.034083.

PKCθ via Activating Transcription Factor 2-mediated CD36 Expression and Foam Cell Formation of Ly6C^{hi} Cells Contributes to Atherosclerosis

Somasundaram Raghavan, PhD[#], **Nikhlesh K. Singh, DVM, PhD**[#], **Sivaiah Gali, MSc**, **Arul M. Mani, PhD**, and **Gadiparthi N. Rao, PhD**

Department of Physiology, University of Tennessee Health Science Center, Memphis, TN 38163, USA

[#] These authors contributed equally to this work.

Abstract

Background: Although the role of thrombin in atherothrombosis is well studied, its role in the pathogenesis of diet-induced atherosclerosis is not known.

Methods: Using a mouse model of diet-induced atherosclerosis and molecular biological approaches, here we have explored the role of thrombin and its G protein-coupled receptor (GPCR) signaling in diet-induced atherosclerosis.

Results: In exploring the role of GPCR signaling in atherogenesis, we found that thrombin triggers foam cell formation via inducing CD36 expression and these events require Par1-mediated Gα12-Pyk2-Gab1-PKCθ-dependent ATF2 activation. Genetic deletion of PKCθ in ApoE$^{-/-}$ mice reduced western diet (WD)-induced plaque formation. Furthermore, thrombin induced Pyk2, Gab1, PKCθ and ATF2 phosphorylation, CD36 expression and foam cell formation in peritoneal macrophages of ApoE$^{-/-}$ mice. On the other hand, thrombin only stimulated Pyk2 and Gab1 but not ATF2 phosphorylation or its target gene CD36 expression in the peritoneal macrophages of ApoE$^{-/-}$:PKCθ$^{-/-}$ mice and it had no effect on foam cell formation. In addition, the aortic root cross sections of WD-fed ApoE$^{-/-}$ mice showed increased Pyk2, Gab1, PKCθ and ATF2 phosphorylation and CD36 expression as compared to ApoE$^{-/-}$:PKCθ$^{-/-}$ mice. Furthermore, while the monocytes from peripheral blood and aorta of WD-fed ApoE$^{-/-}$ mice were found to contain more of Ly6C^{hi} cells than Ly6C^{lo} cells, the monocytes from WD-fed ApoE$^{-/-}$:PKCθ$^{-/-}$ mice were found to contain more of Ly6C^{lo} cells than Ly6C^{hi} cells. Interestingly, the Ly6C^{hi} cells showed higher CD36 expression with enhanced capacity to form foam cells as compared to Ly6C^{lo} cells.

Address for correspondence to: Gadiparthi N. Rao, Ph.D., Department of Physiology, University of Tennessee Health Science Center, 894 Union Avenue, Memphis, TN 38163, Phone: 901-448-7321, Fax: 901-448-7126, rgadipar@uthsc.edu.

AUTHORS CONTRIBUTIONS

SR, performed, RT-PCR, Western blotting, isolation of mouse peritoneal macrophages, foam cell assay, cloning, site-directed mutagenesis, luciferase assay, EMSA, ChIP and Oil Red O staining; NKS, performed Western blotting, isolation of mouse peritoneal macrophages and aortic smooth muscle cells, foam cell assay, enface staining, Oil Red O staining, immunofluorescence, ELISA and FACS; SG, generated ApoE$^{-/-}$:PKCθ$^{-/-}$ mice and performed genotyping; AMM, performed luciferase assays and Western blotting; GN, conceived the overall goal of the project, designed the experiments, interpreted the data and wrote the manuscript.

CONFLICT OF INTEREST

None

Conclusions: The above findings reveal for the first time that thrombin-mediated Par1-Gα12 signaling via targeting Pyk2-Gab1-PKCθ-ATF2-dependent CD36 expression might be playing a crucial role in diet-induced atherogenesis.

Keywords

atherosclerosis; CD36; foam cell; GPCR signaling; macrophages; PKCθ; thrombin

INTRODUCTION

Atherosclerosis is a chronic inflammatory disease of the arterial wall driven by innate and adaptive immune responses and is an intrinsic cause of heart disease and stroke worldwide (1, 2). Inflammatory leukocytes and macrophages are the predominant cells present in the atherosclerotic plaques (3). One of the first indications of vascular complication is endothelial cell dysfunction and leukocyte infiltration (4, 5). These events lead to the trafficking of lymphocytes and monocytes into the arteries (5). Previous observations indicate that circulating monocytes that enter into the arterial intima were further differentiated into foamy macrophages thereby leading to acceleration of atherosclerotic plaques (4). Macrophage buildup within the vascular wall is a salient feature of atherosclerosis (6). However, recent studies have upended this notion by implying that macrophage proliferation within the plaque leads to lesion macrophage buildup (7). Macrophage scavenger receptors are thought to play an important role in atherosclerotic foam cell formation because of their ability to bind and internalize oxidized LDL (oxLDL) (8–11). Macrophages internalize oxLDL through scavenger receptors such as CD36 and are trapped in the arterial intima (12). The interaction between CD36 and oxLDL also induces the secretion of cytokines that recruit additional immune cells into the arterial intima (13) and the arterial inflammation provoked by foam cells induces plaque formation, establishing atherosclerotic lesions (12). Thrombin, a serine protease, which is involved in blood coagulation plays a critical role in the formation of stable clots via activation of platelets and conversion of procofactors to active cofactors leading to cleavage of fibrinogen to fibrin (14). Thrombin is produced at the sites of vascular injury by the interaction of tissue factor with circulating factor VII (15). It was also reported that the expression of factor VII and factor X is increased in macrophages within the atherosclerotic lesions (16). Although many studies have provided ample evidence for the role of the coagulation pathway in atherogenesis and atherothrombosis (17–19), the mechanisms by which thrombin influences atherogenesis are unknown.

Thrombin mediates its effects via its cell surface receptors called protease-activated receptors (Pars) (20). Pars are G protein-coupled receptors (GPCRs) that are uniquely activated by proteolytic cleavage of their N-terminal ends (21). Emerging evidence suggests that thrombin besides its haemostatic effects promotes inflammation and Pars connect its bidirectional effects (22, 23). In fact, a recent study showed that inhibition of thrombin attenuates high fat diet-induced weight gain (24). The presence of Pars in endothelial cells, vascular smooth muscle cells, leukocytes and macrophages may suggest the involvement of thrombin in the pathophysiology of atherosclerosis (20, 21, 23). Protein kinase Cs (PKCs), a serine/threonine protein kinase family of intracellular enzymes, are expressed ubiquitously

in almost all types of cells (25). Many reports have shown that thrombin activates various isoforms of PKCs in several cell types via hydrolysis of multiple phospholipids (26, 27). In addition, it has been shown that leukocyte adhesion, monocyte differentiation and macrophage growth leading to intimal foam cell formation were regulated, in part, through PKC activation (28). Based on this information, we asked the question whether thrombin plays a role in atherogenesis and if it does, does it involve a PKC? Here, we report that thrombin induces CD36 expression and foam cell formation and these events require Gα12-Pyk2-Gab1-PKCθ-dependent ATF2 activation. In addition, genetic deletion of PKCθ attenuates WD-induced ATF2 activation, CD36 expression and foam cell formation resulting in reduced plaque burden in ApoE$^{-/-}$:PKCθ$^{-/-}$ mice as compared to ApoE$^{-/-}$ mice. Interestingly, we found that monocytes from WD-fed ApoE$^{-/-}$:PKCθ$^{-/-}$ mice exhibit Ly6C^{lo} phenotype with reduced CD36 expression and foam cell formation capacity as compared to those from ApoE$^{-/-}$ mice, which were of mainly Ly6C^{hi} phenotype with increased CD36 expression and foam cell formation ability. Together these results infer that thrombin-mediated GPCR signaling plays an important role in diet-induced atherogenesis.

MATERIALS and METHODS

All the materials supporting this study are available from the corresponding author upon request.

The detailed Materials and Methods were provided in the online-only Data Supplement.

Cell culture:

Mouse RAW264.7 macrophage cells were purchased from American Type Culture Collection (Manassas, VA), sub-cultured in DMEM/F-12 medium containing 10% fetal bovine serum and 1X Penicillin/Streptomycin. The cells were quiesced overnight in DMEM/F-12 medium without serum and used between four and ten passages for the experiments.

Animals:

ApoE$^{-/-}$ mice (stock number 002052, Jackson Labs, Bar Harbor, ME) were crossed with PKCθ$^{-/-}$ mice (stock number 005711, Jackson Labs, Bar Harbor, ME) to obtain ApoE$^{-/-}$:PKCθ$^{-/-}$ mice and both the strains were on C57BL/6 background. No phenotypic changes were noticed between ApoE$^{-/-}$ and ApoE$^{-/-}$:PKCθ$^{-/-}$ mice. The F2 littermates were used in the study. Mice were bred and maintained according to the guidelines of the Institutional Animal Care and Use Facility of the University of Tennessee Health Science Center, Memphis, TN. Female and male ApoE$^{-/-}$ and ApoE$^{-/-}$:PKCθ$^{-/-}$ mice were fed with CD or WD (21% fat and 0.2% cholesterol, Harlan Teklad, Harlan Laboratories, Indianapolis, IN) for 16 weeks starting from 8 weeks of age and used for the experiments. The Institutional Animal Care and Use Committee of the University of Tennessee Health Science Center, Memphis, TN, approved all the experiments involving animals.

Statistics:

All the experiments were repeated three times with similar results. Data are presented as the Mean ± S.D. The treatment effects were analyzed by one-way or two-way ANOVA followed

by Tukey's post-hoc test or student's t test and the p values < 0.05 were considered statistically significant. In the case of EMSA, supershift EMSA, ChIP assay, Foam cell, Western blotting and immunofluorescence, one set of the representative data is presented.

RESULTS

Thrombin induces CD36 expression and foam cell formation via PAR1 activation

Accumulation of foam cells of macrophage and smooth muscle cell origin in arteries is an important event in atherogenesis (7, 10). Both macrophages and smooth muscle cells express specialized receptors known as scavenger receptors, which bind and endocytose modified LDL such as oxLDL and thereby involved in foam cell formation (11, 12). Since thrombin generation was reported in atherosclerotic arteries (18, 29), we asked the question whether thrombin has any role in foam cell formation. Thrombin induced foam cell formation of RAW264.7 cells in a time dependent manner (Figure 1A). Since macrophages express several scavenger receptors including SR-A1, SR-B1 and SR-B2 (CD36) (11, 12), we studied the effects of thrombin on the expression of these receptors. Our results show that thrombin induces the expression of CD36 but not SR-A1 or SR-B1 in RAW264.7 cells (Figure 1B). Based on these results we examined the role of CD36 in foam cell formation. Small interference RNA-mediated depletion of CD36 levels reduced foam cell formation (Figure 1C). A large body of evidence shows that thrombin mediates its cellular signaling via activation of Pars in various cell types (20, 21). To identify the Pars involved in thrombin-induced CD36 expression and foam cell formation, we next studied the role of Par1, Par3 and Par4. Depletion of Par1 but not Par3 or Par4 by their respective siRNAs blocked thrombin-induced CD36 expression (Figure 1D). Consistent with these findings, either blockade of Par1 activation by its antagonist SCH79797 (20) or siRNA-mediated depletion of its levels inhibited thrombin-induced foam cell formation (Figure 1E & F).

Activation of Gα12-Pyk2-Gab1 signaling is required for thrombin-induced CD36 expression and foam cell formation

To understand how Par1 mediates the effects of thrombin on CD36 expression and foam cell formation, it is logical to study the role of G proteins, as Par1 is a G protein-coupled receptor (20, 21). Treatment with thrombin caused a rapid dissociation of Gα12 but not Gαq, Gα11 or Gα13 from PAR1, suggesting that thrombin activates Gα12 downstream to Par1 (Figure 2A). Based on these findings, we examined the role of Gα12 in CD36 expression and foam cell formation. Downregulation of Gα12 levels by its siRNA attenuated thrombin-induced CD36 expression and foam cell formation (Figure 2B & C). Previously, we have reported that thrombin induces monocyte migration via Pyk2 activation downstream to Gα12 (30). In view of these observations, we examined the role of Pyk2 in thrombin-induced CD36 expression and foam cell formation. Thrombin induced tyrosine phosphorylation of Pyk2 (Y402) with maximum effect at 1 min (Figure 2D). In addition, pharmacological blockade of Pyk2 by its selective inhibitor PF431396 (31), attenuated thrombin-induced CD36 expression and foam cell formation (Figure 2E & F). Furthermore, inhibition of Par1 by its antagonist SCH79797 or depletion of Gα12 by its siRNA blocked thrombin-induced Pyk2 phosphorylation (Figure 2G & H). Thus, these results demonstrate the involvement of Par1, Gα12 and Pyk2 signaling in thrombin-induced CD36 expression

and foam cell formation. Since we have previously demonstrated that activation of Grb2-associated binder 1 (Gab1) downstream to Gα12 and Pyk2 is required for monocyte migration (30), we next tested its role in CD36 expression and foam cell formation. Thrombin induced tyrosine phosphorylation of Gab1 (Y627) in a time dependent manner with maximum effect at 1 min and siRNA-mediated downregulation of its levels blocked thrombin-induced CD36 expression and foam cell formation (Figure 2I-K). In addition, interference with activation of Par1 or Pyk2 using their antagonists or inhibitors or depletion of Gα12 by its siRNA prevented thrombin-induced Gab1 tyrosine phosphorylation (Figure 2L-N). To ascertain the role of Gα12 in thrombin-induced CD36 expression and foam cell formation, we have examined for the involvement of other G proteins. Depletion of Gαq or Gα11 levels by their siRNAs had no effect on thrombin-induced Pyk2 or Gab1 phosphorylation, CD36 expression or foam cell formation (Supplemental Figure 1). These findings demonstrate that thrombin induces CD36 expression and foam cell formation via activation of Par1, Gα12, Pyk2 and Gab1.

Lack of a role of p115RhoGEF, Rac1, RhoA and Pak2 in thrombin-induced CD36 expression and foam cell formation

Previously we have reported that thrombin induces monocyte migration by activation of Par1-Gα12-Pyk2-Gab1-p115RhoGEF-Rac1-RhoA-Pak2 signaling (30). Based on these observations, we asked the question whether, in addition to Par1, Gα12, Pyk2 and Gab1, activation of p115RhoGEF, Rac1, RhoA or Pak2 is required for thrombin-induced CD36 expression and foam cell formation. Consistent with our previous observations, thrombin induced p115RhoGEF, Rac1, RhoA and Pak2 activation as measured by their tyrosine or serine/threonine phosphorylation or pull-down assay (Figure 3A). In lieu of these observations, we next tested their role in thrombin-induced CD36 expression and foam cell formation. Depletion of p115RhoGEF, Rac1, RhoA or Pak2 had no effect on thrombin-induced CD36 expression and foam cell formation (Figure 3B-I). These findings infer that while Par1, Gα12, Pyk2 and Gab1 activation is required for thrombin-induced CD36 expression and foam cell formation, the activation of p115RhoGEF, Rac1, RhoA or Pak2 was not needed for these effects.

PKCθ mediates thrombin-induced CD36 expression and foam cell formation

Since many reports have shown a role for various PKC isozymes in CD36 expression (32), we examined the role of PKCs in thrombin-induced CD36 expression and foam cell formation. While having no major effects on PKCγ (T514), ε, η and ζ (T410/403), thrombin activated PKCα/βII (T638/641), δ (T505), and θ (T538) in a time dependent manner in RAW264.7 cells (Figure 4A). However, as activation of PKCθ precedes CD36 expression we speculated a possible role for this PKC isozyme in thrombin-induced CD36 expression and foam cell formation. Indeed, down regulation of PKCθ by its siRNA substantially blocked thrombin-induced CD36 expression and foam cell formation (Figure 4B & C). To find the upstream mechanisms of its activation, we tested the role of Par1, Gα12, Pyk2 and Gab1. As shown in Figure 4D-G, pharmacological interference with Par1 or Pyk2 activation or siRNA-mediated depletion of Gα12 or Gab1 levels blocked thrombin-induced PKCθ phosphorylation (Figure 4D-G). Together these results infer that thrombin-

induced CD36 expression and foam cell formation depends on Par1, Gα12, Pyk2 and Gab1-dependent PKCθ activation.

ATF2 activation downstream to PAR1, Gα12, Pyk2 Gab1 and PKCθ is essential for thrombin-induced CD36 expression and foam cell formation

Previous studies have shown that PPARγ plays a role in CD36 expression (12). To find whether thrombin-induced CD36 expression requires PPARγ, we tested the time course effect of thrombin on PPARγ activation. Thrombin had no effect on either the steady state levels or phosphorylation or acetylation of PPARγ (Figure 5A). This may indicate a lack of a role for PPARγ in thrombin-induced CD36 expression. Some reports showed that oxLDL induces CD36 expression via JNK-mediated phosphorylation of activating transcription factor 2 (ATF2), a leucine zipper transcriptional factor (33). Since not much is known on the role of ATF2 in CD36 expression and foam cell formation and its activation depends on its serine phosphorylation, we hypothesized that thrombin could induce CD36 expression through activation of ATF2. Indeed, our results show that thrombin stimulates ATF2 phosphorylation (T71) in a time dependent manner (Figure 5B). Furthermore, siRNA-mediated downregulation of ATF2 levels suppressed thrombin-induced CD36 expression and foam cell formation (Figure 5C & D). In addition, inhibition of either Par1 or Pyk2 or depletion of Gα12, Gab1 or PKCθ levels attenuated thrombin-induced ATF2 phosphorylation (Figure 5E-I). To confirm the role of Par1 in thrombin-induced Pyk2, Gab1, PKCθ and ATF2 activation, CD36 expression and foam cell formation, we tested the effect of Par1 activating peptide TFLLRN. Indeed, TFLLRN stimulated Pyk2, Gab1, PKCθ and ATF2 phosphorylation, CD36 expression and foam cell formation (Supplemental Figure 2). These results further substantiate the role of Par1 in thrombin-induced CD36 expression and foam cell formation. To identify the regulatory elements through which thrombin induces CD36 expression, we cloned a 0.8 kb region of CD36 promoter and by applying TRANSFAC analysis identified one putative ATF2 binding site at -100 nt from the transcription start site (Figure 5J). Furthermore, the promoter-luciferase reporter gene assays indicated that thrombin induces CD36 promoter activity and site-directed mutagenesis of the ATF2-binding site at -100 nt (from TGACCTCT to TGA**TA**T**T**T; mutations were shown in bold letters) blunts this effect (Figure 5K & L). In addition, interference with Par1 or Pyk2 activation or depletion of Gab1, PKCθ or ATF2 levels reduced thrombin-induced CD36 promoter activity (Figure 5M & N). The EMSA, supershift EMSA and ChIP assays further revealed that ATF2 binds to CD36 promoter in response to thrombin (Figure 5O-Q). To confirm our observations on the effects of thrombin in RAW264.7 cells, we also studied its effects on PKCθ and ATF2 phosphorylation and CD36 expression in primary peritoneal macrophages of C57BL/6 mice. Thrombin induced PKCθ and ATF2 phosphorylation and CD36 expression robustly in these cells as well (Figure 5R).

PKCθ plays an essential role in diet-induced atherosclerosis

To test the role of PKCθ in atherosclerosis we cross-bred PKCθ$^{-/-}$ with ApoE$^{-/-}$ mice to generate ApoE$^{-/-}$:PKCθ$^{-/-}$ on C57BL/6 background. The F2 littermates of ApoE$^{-/-}$ and ApoE$^{-/-}$:PKCθ$^{-/-}$ mice were fed with WD starting from 8 weeks of age to 24 weeks of age and analyzed for atheroma formation. Although no significant differences were found in the body weight, total cholesterol, HDL and LDL levels between CD-fed or WD-fed ApoE$^{-/-}$

and ApoE$^{-/-}$:PKCθ$^{-/-}$ mice, ApoE$^{-/-}$:PKCθ$^{-/-}$ mice showed decreased plasma triglyceride levels as compared to ApoE$^{-/-}$ mice that were fed with either CD or WD (Table 1). Measurement of total atherosclerotic lesion area by en face staining revealed a significant decrease in the lesions in the aorta of ApoE$^{-/-}$:PKCθ$^{-/-}$ mice as compared to ApoE$^{-/-}$ mice (Figure 6A). The percentage of plaque area in the aortic roots of WD-fed ApoE$^{-/-}$:PKCθ$^{-/-}$ mice was also decreased significantly as compared to ApoE$^{-/-}$ mice (Figure 6B). To validate the role of PKCθ in CD36 expression in vivo and to test the role of Par1-dependent Gα12-mediated Pyk2, Gab1, PKCθ and ATF2 signaling activation on these effects, we studied the influence of diet on the stimulation of this signaling cascade in the primary peritoneal macrophages of ApoE$^{-/-}$ and ApoE$^{-/-}$:PKCθ$^{-/-}$ mice. We found that Pyk2 and Gab1 were activated in the primary peritoneal macrophages of WD-fed ApoE$^{-/-}$ and ApoE$^{-/-}$:PKCθ$^{-/-}$ mice as compared to CD-fed ApoE$^{-/-}$ mice (Figure 6C). However, ATF2 activation and CD36 expression were seen only in WD-fed ApoE$^{-/-}$ mice but not ApoE$^{-/-}$:PKCθ$^{-/-}$ mice as compared to CD-fed ApoE$^{-/-}$ mice (Figure 6C). To obtain additional line of evidence, we also studied the effects of thrombin on the activation of Par1, Gα12, Pyk2, Gab1, PKCθ and ATF2 leading to CD36 expression and foam cell formation in the primary peritoneal macrophages of ApoE$^{-/-}$ versus ApoE$^{-/-}$:PKCθ$^{-/-}$ mice ex vivo. The time course results showed that thrombin induces Gα12 dissociation from Par1, activates Pyk2, Gab1, PKCθ and ATF2 as measured by their phosphorylation and induces CD36 expression in the primary peritoneal macrophages of ApoE$^{-/-}$ mice (Figure 6D). On the other hand, thrombin while stimulating the dissociation of Gα12 from Par1 and increasing the phosphorylation of Pyk2 and Gab1 had no effect on PKCθ or ATF2 phosphorylation or CD36 expression in the primary peritoneal macrophages of ApoE$^{-/-}$:PKCθ$^{-/-}$ mice (Figure 6D). Since thrombin stimulated PKCα/βII in Raw264.7 cells, we wanted to find whether this PKC isozyme plays a compensatory role for the loss of PKCθ. Thrombin stimulated PKCα/βII in the primary peritoneal macrophages of both ApoE$^{-/-}$ and ApoE$^{-/-}$:PKCθ$^{-/-}$ mice to a similar extent, suggesting no compensatory role for it (Figure 6D). In line with these observations, thrombin induced the foam cell formation only in the primary peritoneal macrophages of ApoE$^{-/-}$ but not ApoE$^{-/-}$:PKCθ$^{-/-}$ mice (Figure 6E). To link ATF2 activation to CD36 expression and foam cell formation, we used siRNA approach. Depletion of ATF2 levels substantially reduced CD36 expression and foam cell formation in peritoneal macrophages of ApoE$^{-/-}$ mice (Figure 6F). To understand whether ATF2 modulates macrophage proliferation in the development of atherosclerosis, we tested the effect of ATF2 depletion on macrophage growth. Depletion of ATF2 had no effect on macrophage proliferation (Figure 6G). We next examined these signaling molecules in the aortic root cross sections of WD-fed ApoE$^{-/-}$ and ApoE$^{-/-}$:PKCθ$^{-/-}$ mice. Immunofluorescence staining of the aortic root cross sections showed increased Pyk2, Gab1, PKCθ and ATF2 phosphorylation and CD36 expression and their colocalization with Mac3 in ApoE$^{-/-}$ mice as compared to ApoE$^{-/-}$:PKCθ$^{-/-}$ mice in response to WD feeding (Figure 6H). These observations correlate with our in vitro results and confirm that thrombin-induced CD36 expression and foam cell formation occur via Par1-Gα12-Pyk2-Gab1-PKCθ-mediated activation of ATF2. Since SMCs also play a role in foam cell formation during atherogenesis (10–12), we asked the question whether thrombin triggers a similar signaling axis of CD36 expression in these cells. It is indeed exciting to find that thrombin induces PKCθ and ATF2 phosphorylation as

well as CD36 expression in SMCs isolated from ApoE$^{-/-}$ but not ApoE$^{-/-}$:PKCθ$^{-/-}$ mice (Figure 6I).

PKCθ skews monocyte differentiation towards Ly6C^{hi} phenotype and enhances foam cell formation

Since atherosclerotic lesions were reduced in the aortic root and aorta of WD-fed ApoE$^{-/-}$:PKCθ$^{-/-}$ mice as compared to ApoE$^{-/-}$, we were intrigued to find whether PKCθ might be involved in the regulation of monocyte differentiation. To test this, we have determined the monocyte subtypes in the peripheral blood and aorta of WD-fed ApoE$^{-/-}$ and ApoE$^{-/-}$:PKCθ$^{-/-}$ mice. We characterized the phenotype of the monocytes in these mice based on the following four subpopulations as Ly6C^{hi}F4/80^{lo}CD11c^{lo}I-Ab^{lo}, Ly6C^{hi}F4/80^{hi}CD11c^{hi}I-Ab^{hi}, Ly6C^{lo}F4/80^{hi}CD11c^{hi}I-Ab^{hi} and Ly6C^{lo}F4/80^{lo}CD11c^{lo}I-Ab^{lo}. We found that the number of pro-inflammatory Ly6C^{hi} monocytes were substantially lower in both the peripheral blood and aorta of ApoE$^{-/-}$:PKCθ$^{-/-}$ mice as compared to ApoE$^{-/-}$ mice (Figure 7A-D). In contrast, the number of Ly6C^{lo} monocytes were found to be substantially higher in the peripheral blood and aorta of ApoE$^{-/-}$:PKCθ$^{-/-}$ mice as compared to ApoE$^{-/-}$ mice (Figure 7A-D). Since macrophages by taking up modified LDL become foam cells and lipid-laden foam cell accumulation is a hallmark of atherosclerosis (11, 12), we wanted to find which of these monocytes possess such capacity. It is interesting to note that Ly6C^{hi} monocytes were found to express substantially higher levels of CD36 and possess more capacity to form foam cells as compared to Ly6C^{lo} cells (Figure 7E). To find whether genetic deletion of PKCθ affects the balance between pro and anti-inflammatory cytokine levels, we measured plasma cytokine levels in WD-fed ApoE$^{-/-}$ and ApoE$^{-/-}$:PKCθ$^{-/-}$ mice. No major differences were observed in the pro- and anti-inflammatory cytokine levels between ApoE$^{-/-}$ and ApoE$^{-/-}$:PKCθ$^{-/-}$ mice (Figure 7F).

DISCUSSION

A large body of evidence shows that atherosclerotic events are triggered by the disparity between cholesterol metabolism and inflammatory response leading to accumulation of lipid-loaded macrophages and SMCs in the arterial wall (34–36). Among the many cell types such as dendritic cells, lymphocytes, monocytes and SMCs present in atherosclerotic plaques, monocyte-derived macrophages and SMCs are of immense importance due to their ability to become cholesterol-laden foam cells, which is the major contributing factor of atherosclerosis (37). Scavenger receptors such as CD36, SR-A1 and SR-B1 have been shown to play a crucial role in oxLDL uptake and foam cell formation in rodent atherosclerotic models (38, 39). Thrombin, which is a major platelet activator, has been shown to contribute to atherogenesis in a platelet-independent manner, although the underlying mechanisms were not known (40). Previous studies from our laboratory have shown that thrombin modulates monocyte and SMC migration via activation of Par1-Gα12-Pyk2-Gab1-p115RhoGEF-Rac1-RhoA and Pak2/Pak1 signaling (30, 41). In this study we found that thrombin selectively induces CD36 expression and facilitates foam cell formation of RAW264.7 cells through activation of Par1-Gα12-Pyk2-Gab1 signaling. Interestingly, thrombin-induced CD36 expression and foam cell formation were not affected when p115RhoGEF, Rac1, RhoA or Pak2 levels were depleted, suggesting a lack of a role for

these molecules in CD36 expression and foam cell formation. These results may infer that while thrombin-induced CD36 expression and foam cell formation requires Par1-Gα12-Pyk2-Gab1 signaling, activation of p115RhoGEF, Rac1, RhoA or Pak2 is not essential. It also infers that thrombin-induced CD36 expression and foam cell formation diverge at the level of Gab1, which is an adopter molecule (42).

Previous studies have shown that TNFα inhibits cholesterol efflux via downregulation of ABCA1, ABCG1 and LXRα and upregulation of CD36 and SR-A expression through activation of PKCθ (43). In addition, it has been shown that inhibition of PKC signaling by PKC inhibitory peptides or siRNA for PKCα and PKCβ but not PKCδ, PKCε or PKCθ results in the secretion of ApoE and clearance of the triglyceride-rich lipoprotein, and cholesterol efflux from foam cells (44). Thus differential roles of PKCs in atherosclerosis were reported. In this regard, our results show that thrombin activates PKCθ in mediating CD36 expression and foam cell formation. More importantly, inhibition of Par1, Gα12, Pyk2 or Gab1 led to downregulation of PKCθ activation. Taken together, these results suggest that PKCθ acts downstream to Par1-Gα12-Pyk2-Gab1 signaling in CD36 expression and foam cell formation. Our results further reveal that thrombin-induced CD36 expression and foam cell formation require ATF2 activation downstream to PKCθ in both RAW264.7 cells and primary peritoneal macrophages of WT mice. Interestingly, ATF2 appears to be essential for CD36 expression and foam cell formation as mutation of its binding element at -100 nt in CD36 promoter almost completely abolished CD36 promoter activity. To confirm the role of PKCθ-ATF2 axis in CD36 expression and foam cell formation in vivo, we observed decreased plaque burden in $ApoE^{-/-}$:$PKC\theta^{-/-}$ mice as compared to $ApoE^{-/-}$ mice fed with WD. We also found that while thrombin activates Gα12, Pyk2, and Gab1 in peritoneal macrophages of both $ApoE^{-/-}$ and $ApoE^{-/-}$:$PKC\theta^{-/-}$ mice, it had no effect on ATF2 phosphorylation and CD36 expression in $ApoE^{-/-}$:$PKC\theta^{-/-}$ mice. In addition, depletion of ATF2 levels attenuated thrombin-induced CD36 expression and foam cell formation in primary peritoneal macrophages of $ApoE^{-/-}$ mice. Interestingly, the role of PKCθ-ATF2 signaling axis in CD36 expression and foam cell formation appears to be a predominant mechanism in GPCR signaling-mediated foam cell formation, as thrombin activated this signaling axis in SMCs of $ApoE^{-/-}$ mice but not in $ApoE^{-/-}$:$PKC\theta^{-/-}$ mice. These results conclude that ATF2 is the effector molecule of PKCθ in the regulation of CD36 expression and foam cell formation both in macrophages and SMCs. Since, plasma triglyceride levels were significantly lower in $ApoE^{-/-}$:$PKC\theta^{-/-}$ mice as compared to $ApoE^{-/-}$ mice fed with CD or WD, it is likely that besides its role in WD-induced CD36 expression and foam cell formation, PKCθ may also be involved in the modulation of plasma triglyceride levels.

A growing body of evidence demonstrates that in addition to macrophage numbers, an altered phenotype of macrophages towards inflammatory lineage is associated with the progression of atherosclerosis in animal models (45–47). We found that monocytes isolated from peripheral blood and aorta of $ApoE^{-/-}$:$PKC\theta^{-/-}$ mice mostly were of $Ly6C^{lo}$ phenotype whereas the monocytes from $ApoE^{-/-}$ mice were predominantly of $Ly6C^{hi}$ phenotype. These findings reveal that PKCθ could enhance inflammation in response to WD feeding and thereby influence atherogenesis, as $Ly6C^{hi}$ monocytes are linked to disease progression and $Ly6C^{lo}$ monocytes are associated with disease regression (45, 48). Indeed, our present

findings also reveal that Ly6C^{hi} monocytes express more levels of CD36 expression and possess higher capacity to form foam cells than Ly6C^{lo} monocytes. Thus, we show for the first time that PKCθ via mediating CD36 expression, thereby increasing the capacity of macrophages to form foam cells plays a crucial role in atherosclerosis. Previous studies have shown that deletion of PKCθ improves insulin sensitivity (49). Since diabetes is a risk factor for cardiovascular diseases (28) it is possible that PKCθ could be a common signaling molecule involved both in diabetes and atherosclerosis. Therefore, PKCθ could be a potential target for the development of therapeutics against atherosclerosis. In addition, emerging evidence reveals a role for thrombin in the modulation of non-haemostatic effects such as inflammation and that it exerts a critical axis in the development of atherosclerosis (22, 23), although there is no proof of evidence for its involvement in atherosclerosis. In this regard, the present findings also provide the first evidence for the possible role of thrombin and perhaps its receptor Par1 and its downstream signaling in foam cell formation and atherosclerosis. The possibility may also exist that thrombin could influence foam cell formation thereby atherogenesis not only by enhancing the uptake of modified LDL but also by decreasing the cholesterol efflux. The increased generation of thrombin during early development of atherosclerosis in animal models (50) further lends support for its role in diet-induced atherogenesis.

Supplementary Material

Refer to Web version on PubMed Central for supplementary material.

Acknowledgments

SOURCES OF FUNDING

This work was supported in part by National Heart, Lung and Blood Institute of NIH (grant HL103575 to Dr. Rao).

REFERENCES

1. Ait-Oufella H, Taleb S, Mallat Z, Tedgui A. Recent advances on the role of cytokines in atherosclerosis. Arterioscler Thromb Vasc Biol. 2011;31:969–979. [PubMed: 21508343]
2. Lusis AJ. Atherosclerosis. Nature. 2000;407:233–241. [PubMed: 11001066]
3. Galkina E, Ley K. Immune and inflammatory mechanisms of atherosclerosis. Annu Rev Immunol. 2009;27:165–197. [PubMed: 19302038]
4. Gerrity RG. The role of the monocyte in atherogenesis: II. Migration of foam cells from atherosclerotic lesions. Amer J Pathol. 1981;103:191–200. [PubMed: 7234962]
5. Libby P Inflammation in atherosclerosis. Nature. 2002;420:868–874. [PubMed: 12490960]
6. Chinetti-Gbaguidi G, Colin S, and Staels B. Macrophage subsets in atherosclerosis. Nat Rev Cardiol. 2015;12:10–17. [PubMed: 25367649]
7. Robbins CS, Hilgendorf I, Weber GF, Theurl I, Iwamoto Y, Figueiredo JL, Gorbatov R, Sukhova GK, Gerhardt LM, Smyth D, Zavitz CC, Shikatani EA, Parsons M, van Rooijen N, Lin HY, Husain M, Libby P, Nahrendorf M, Weissleder R, Swirski FK. Local proliferation dominates lesional macrophage accumulation in atherosclerosis. Nat Med. 2013;19:1166–1172. [PubMed: 23933982]
8. Lipoproteins Steinberg D. and the pathogenesis of atherosclerosis. Circulation. 1987;76:508–514. [PubMed: 3621517]
9. Steinberg D, Parthasarathy S, Carew TE, Khoo JC, Witztum JL. Beyond cholesterol. Modifications of low-density lipoprotein that increase its atherogenicity. N Engl J Med. 1989;320:915–924. [PubMed: 2648148]

10. Gown AM, Tsukada T, Ross R. Human atherosclerosis. II. Immunocytochemical analysis of the cellular composition of human atherosclerotic lesions. Amer J Pathol. 1986;125:191–207. [PubMed: 3777135]
11. Fogelman AM, Van Lenten BJ, Warden C, Haberland ME, Edwards PA. Macrophage lipoprotein receptors. J Cell Sci. 1988;9:135–149.
12. Collot-Teixeira S, Martin J, McDermott-Roe C, Poston R, McGregor JL. CD36 and macrophages in atherosclerosis. Cardiovasc Res. 2007;75:468–477. [PubMed: 17442283]
13. Jiang Y, Wang M, Huang K, Zhang Z, Shao N, Zhang Y, Wang W, Wang S. Oxidized low-density lipoprotein induces secretion of interleukin-1beta by macrophages via reactive oxygen species-dependent NLRP3 inflammasome activation. Biochem Biophys Res Commun. 2012;425:121–126. [PubMed: 22796220]
14. Huntington JA. Natural inhibitors of thrombin. Thromb Haemost. 2014;111:583–589. [PubMed: 24477356]
15. Hackeng TM, Maurissen LF, Castoldi E, Rosing J. Regulation of TFPI function by protein S. J Thromb Haemost. 2009;7:165–168. [PubMed: 19630792]
16. Wilcox JN, Noguchi S, Casanova JR, Rasmussen ME. Extrahepatic synthesis of FVII in human atheroma and smooth muscle cells in vitro. Ann N Y Acad Sci. 2001;947:433–438. [PubMed: 11795309]
17. Coughlin SR. Protease-activated receptors in hemostasis, thrombosis and vascular biology. J Thromb Haemost. 2005;3:1800–1814. [PubMed: 16102047]
18. Grandoch M, Kohlmorgen C, Melchior-Becker A, Feldmann K, Homann S, Müller J, Kiene LS, Zeng-Brouwers J, Schmitz F, Nagy N, Polzin A, Gowert NS, Elvers M, Skroblin P, Yin X, Mayr M, Schaefer L, Tannock LR, Fischer JW. Loss of Biglycan Enhances Thrombin Generation in Apolipoprotein E-Deficient Mice: Implications for Inflammation and Atherosclerosis. Arterioscler Thromb Vasc Biol. 2016;36:e41–50. [PubMed: 27034473]
19. Vendrov AE, Madamanchi NR, Hakim ZS, Rojas M, Runge MS. Thrombin and NAD(P)H oxidase-mediated regulation of CD44 and BMP4-Id pathway in VSMC, restenosis, and atherosclerosis. Circ Res. 2006;98:1254–1263. [PubMed: 16601225]
20. Macfarlane SR, Seatter MJ, Kanke T, Hunter GD, Plevin R. Proteinase-activated receptors. Pharmacological Rev. 2001;53:245–282.
21. Ossovskaya VS, Bunnett NW. Protease-activated receptors: contribution to physiology and disease. Physiol Rev. 2004;84:579–621. [PubMed: 15044683]
22. Borissoff JI, Spronk HM, ten Cate H. The hemostatic system as a modulator of atherosclerosis. N Engl J Med. 2011;364:1746–1760. [PubMed: 21542745]
23. Esmon CT. Targeting factor Xa and thrombin: impact on coagulation and beyond. Thromb Haemost 2014;111:625–633. [PubMed: 24336942]
24. Kopec AK, Joshi N, Towery KL, Kassel KM, Sullivan BP, Flick MJ, Luyendyk JP. Thrombin inhibition with dabigatran protects against high-fat diet-induced fatty liver disease in mice. J Pharmacol Exp Ther. 2014;351:288–297. [PubMed: 25138021]
25. Steinberg SF. Structural basis of protein kinase C isoform function. Physiol Rev. 2008;88:1341–1378. [PubMed: 18923184]
26. Ha KS, Exton JH. Differential translocation of protein kinase C isozymes by thrombin and platelet-derived growth factor. A possible function for phosphatidylcholine-derived diacylglycerol. J Biol Chem. 1993;268:10534–10539. [PubMed: 8486706]
27. Minshall RD, Vandenbroucke EE, Holinstat M, Place AT, Tiruppathi C, Vogel SM, van Nieuw Amerongen GP, Mehta D, Malik AB. Role of protein kinase Czeta in thrombin-induced RhoA activation and inter-endothelial gap formation of human dermal microvessel endothelial cell monolayers. Microvasc Res. 2010;80:240–249. [PubMed: 20417648]
28. Rask-Madsen C, King GL. Proatherosclerotic mechanisms involving protein kinase C in diabetes and insulin resistance. Arterioscler Thromb Vasc Biol. 2005;25:487–496. [PubMed: 15637306]
29. Iwaki T, Sandoval-Cooper MJ, Brechmann M, Ploplis VA, Castellino FJ. A fibrinogen deficiency accelerates the initiation of LDL cholesterol-driven atherosclerosis via thrombin generation and platelet activation in genetically predisposed mice. Blood. 2006;107:3883–3891. [PubMed: 16434491]

30. Gadepalli R, Kotla S, Heckle MR, Verma SK, Singh NK, Rao GN. Novel role for p21-activated kinase 2 in thrombin-induced monocyte migration. J Biol Chem. 2013;288:30815–30831. [PubMed: 24025335]

31. Buckbinder L, Crawford DT, Qi H, Ke HZ, Olson LM, Long KR, Bonnette PC, Baumann AP, Hambor JE, Grasser WA, 3rd, Pan LC, Owen TA, Luzzio MJ, Hulford CA, Gebhard DF, Paralkar VM, Simmons HA, Kath JC, Roberts WG, Smock SL, Guzman-Perez A, Brown TA, Li M. Proline-rich tyrosine kinase 2 regulates osteoprogenitor cells and bone formation, and offers an anabolic treatment approach for osteoporosis. Proc Natl Acad Sci U S A. 2007;104:10619–10624. [PubMed: 17537919]

32. Lin CS, Lin FY, Ho LJ, Tsai CS, Cheng SM, Wu WL, Huang CY, Lian CH, Yang SP, Lai JH. PKCδ signalling regulates SR-A and CD36 expression and foam cell formation. Cardiovasc Res. 2012;95:346–355. [PubMed: 22687273]

33. Rahaman SO, Lennon DJ, Febbraio M, Podrez EA, Hazen SL, and Silverstein RL. A CD36-dependent signaling cascade is necessary for macrophage foam cell formation. Cell Metabolism. 2006;4:211–221. [PubMed: 16950138]

34. Feig JE, Parathath S, Rong JX, Mick SL, Vengrenyuk Y, Grauer L, Young SG, Fisher EA. Reversal of hyperlipidemia with a genetic switch favorably affects the content and inflammatory state of macrophages in atherosclerotic plaques. Circulation. 2011;123:989–998. [PubMed: 21339485]

35. Moore KJ, Tabas I. Macrophages in the pathogenesis of atherosclerosis. Cell. 2011;145:341–355. [PubMed: 21529710]

36. Randolph GJ. Emigration of monocyte-derived cells to lymph nodes during resolution of inflammation and its failure in atherosclerosis. Curr Opin Lipidol. 2008;19:462–468. [PubMed: 18769227]

37. Moore KJ, Sheedy FJ, Fisher EA. Macrophages in atherosclerosis: a dynamic balance. Nat Rev Immunol. 2013;13:709–721. [PubMed: 23995626]

38. Febbraio M, Hajjar DP, Silverstein RL. CD36: a class B scavenger receptor involved in angiogenesis, atherosclerosis, inflammation, and lipid metabolism. J Clin Invest. 2001;108:785–791. [PubMed: 11560944]

39. de Winther MP, van Dijk KW, Havekes LM, Hofker MH. Macrophage scavenger receptor class A: A multifunctional receptor in atherosclerosis. Arterioscler Thromb Vasc Biol. 2000;20:290–297. [PubMed: 10669623]

40. Hamilton JR, Cornelissen I, Mountford JK, Coughlin SR. Atherosclerosis proceeds independently of thrombin-induced platelet activation in ApoE-/- mice. Atherosclerosis. 2009;205:427–432. [PubMed: 19217621]

41. Gadepalli R, Singh NK, Kundumani-Sridharan V, Heckle MR, Rao GN. Novel role of proline-rich nonreceptor tyrosine kinase 2 in vascular wall remodeling after balloon injury. Arterioscler Thromb Vasc Biol. 2012;32:2652–61. [PubMed: 22922962]

42. Takahashi-Tezuka M, Yoshida Y, Fukada T, Ohtani T, Yamanaka Y, Nishida K, Nakajima K, Hibi M, Hirano T. Gab1 acts as an adapter molecule linking the cytokine receptor gp130 to ERK mitogen-activated protein kinase. Mol Cell Biol. 1998;18:4109–4117. [PubMed: 9632795]

43. Ma AZ, Zhang Q, Song ZY. TNFα alter cholesterol metabolism in human macrophages via PKCθ-dependent pathway. BMC Biochem. 2013;14:20. [PubMed: 23914732]

44. Karunakaran D, Kockx M, Owen DM, Burnett JR, Jessup W, Kritharides L. Protein kinase C controls vesicular transport and secretion of apolipoprotein E from primary human macrophages. J Biol Chem. 2013;288:5186–5197. [PubMed: 23288845]

45. Swirski FK, Libby P, Aikawa E, Alcaide P, Luscinskas FW, Weissleder R, Pittet MJ. Ly-6Chi monocytes dominate hypercholesterolemia-associated monocytosis and give rise to macrophages in atheromata. J Clin Invest. 2007;117:195–205. [PubMed: 17200719]

46. Combadiere C, Potteaux S, Rodero M, Simon T, Pezard A, Esposito B, Merval R, Proudfoot A, Tedgui A, Mallat Z. Combined inhibition of CCL2, CX3CR1, and CCR5 abrogates Ly6C(hi) and Ly6C(lo) monocytosis and almost abolishes atherosclerosis in hypercholesterolemic mice. Circulation. 2008;117:1649–1657. [PubMed: 18347211]

47. Libby P, Tabas I, Fredman G, Fisher EA. Inflammation and its resolution as determinants of acute coronary syndromes. Circ Res. 2014;114:1867–1879. [PubMed: 24902971]

48. Li X, Wang D, Chen Z, Lu E, Wang Z, Duan J, Tian W, Wang Y, You L, Zou Y, Cheng Y, Zhu Q, Wan X, Xi T, Birnbaumer L, Yang Y. Gαi1 and Gαi3 regulate macrophage polarization by forming a complex containing CD14 and Gab1. Proc Natl Acad Sci U S A. 2015;112:4731–4736. [PubMed: 25825741]

49. Kim JK, Fillmore JJ, Sunshine MJ, Albrecht B, Higashimori T, Kim DW, Liu ZX, Soos TJ, Cline GW, O'Brien WR, Littman DR, Shulman GI. PKC-theta knockout mice are protected from fat-induced insulin resistance. J Clin Invest. 2004;114:823–827. [PubMed: 15372106]

50. Kalz J, ten Cate H, Spronk HM. Thrombin generation and atherosclerosis. J Thromb Thrombolysis. 2014;37:45–55. [PubMed: 24241912]

CLINICAL PERSPECTIVE

What Is New?

- In addition to its essential role in platelet activation and thrombosis, in the present study we demonstrate for the first time that thrombin-GPCR signaling plays a role in diet-induced atherogenesis.
- Thrombin-induced CD36 expression and foam cell formation require Par1, Gα12, Pyk2, Gab1 and PKCθ-dependent ATF2 activation.
- $Ly6C^{hi}$ cells appear to be the predominant inflammatory cells that take up modified LDL and contribute to the accumulation of lipid-laden foam cells in the development of atherosclerosis.

What are the Clinical Implications?

- Inhibition of thrombin-GPCR signaling could be a promising target for the development of drugs in reducing the risk of diet-induced atherogenesis.
- Since inhibition of PKCθ decreases atherosclerotic lesions and improves insulin sensitivity, this PKC isozyme could be a potential target for the treatment of diabetes and atherosclerosis.

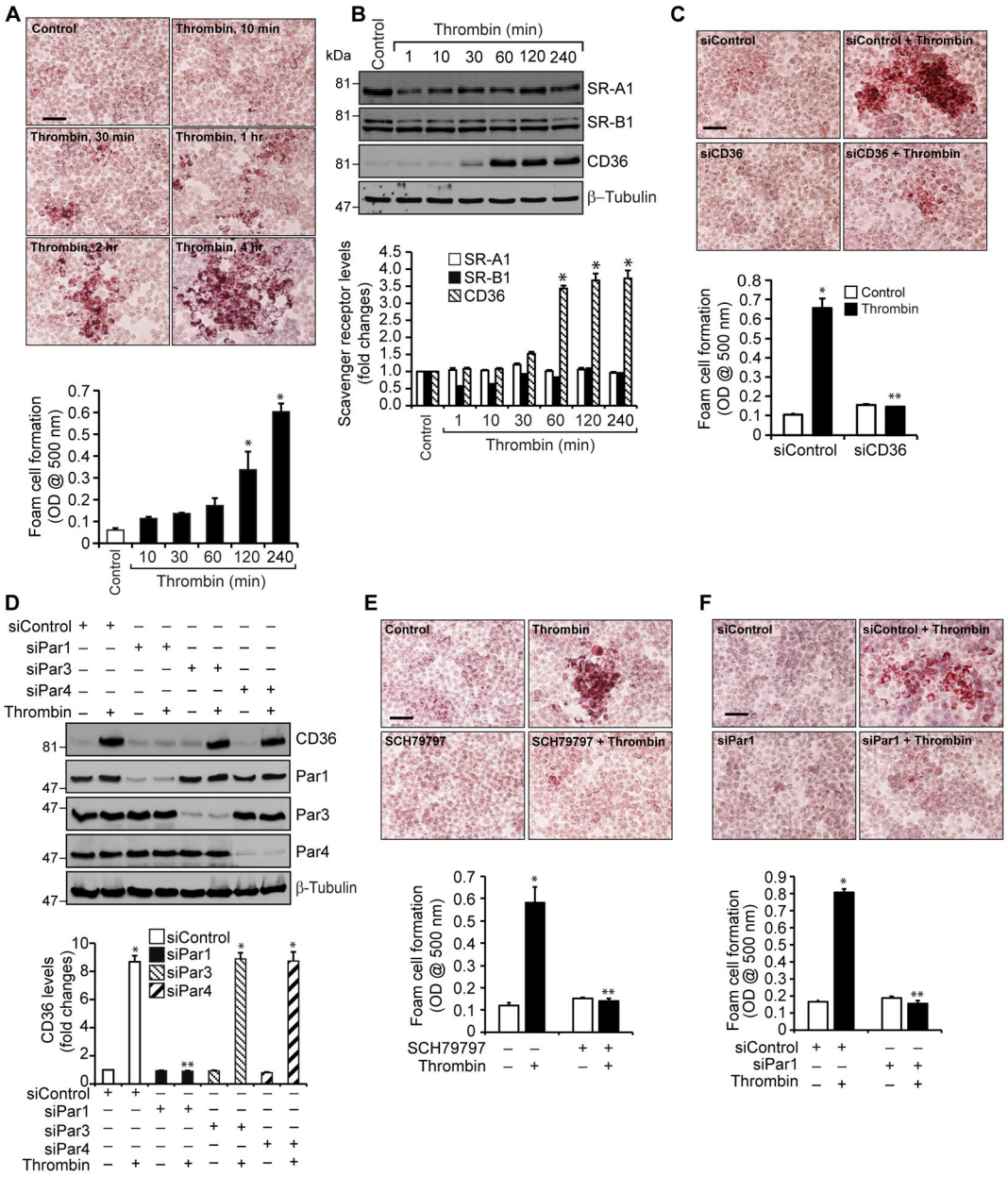

Figure 1. Thrombin induces CD36 expression and foam cell formation via Par1 activation.

A. Quiescent RAW264.7 cells were treated with or without thrombin (0.5 U/ml) for the indicated time periods and analyzed for foam cell formation. B. Equal amounts of protein from control and the indicated time periods of thrombin-treated cells were analyzed by Western blotting for SR-A1, SR-B1 and CD36 levels and normalized to β-tubulin. C. Cells were transfected with siControl or siCD36 (100 nM), quiesced, treated with and without thrombin for 4 hrs and analyzed for foam cell formation. D. Cells were transfected with siControl, siPar1, siPar3 or siPar4 (100 nM), quiesced, treated with and without thrombin for 1 hr and analyzed by Western blotting for CD36 levels and the blot was reprobed for Par1, Par3, Par4 or β-tubulin levels to show the effect of the siRNA on its target and off target molecules levels. E. Quiescent cells were treated with and without thrombin in the presence

and absence of SCH79797 (10 μM) for 4 hrs and analyzed for foam cell formation. F. Cells were transfected with siControl or siPar1 (100 nM), quiesced, treated with and without thrombin for 4 hrs and analyzed for foam cell formation. The bar graphs represent Mean ± S.D. values of three experiments. *, $p < 0.05$ vs control or siControl; **, $p < 0.05$ vs Thrombin or siControl + Thrombin. Scale bar is 50 μm.

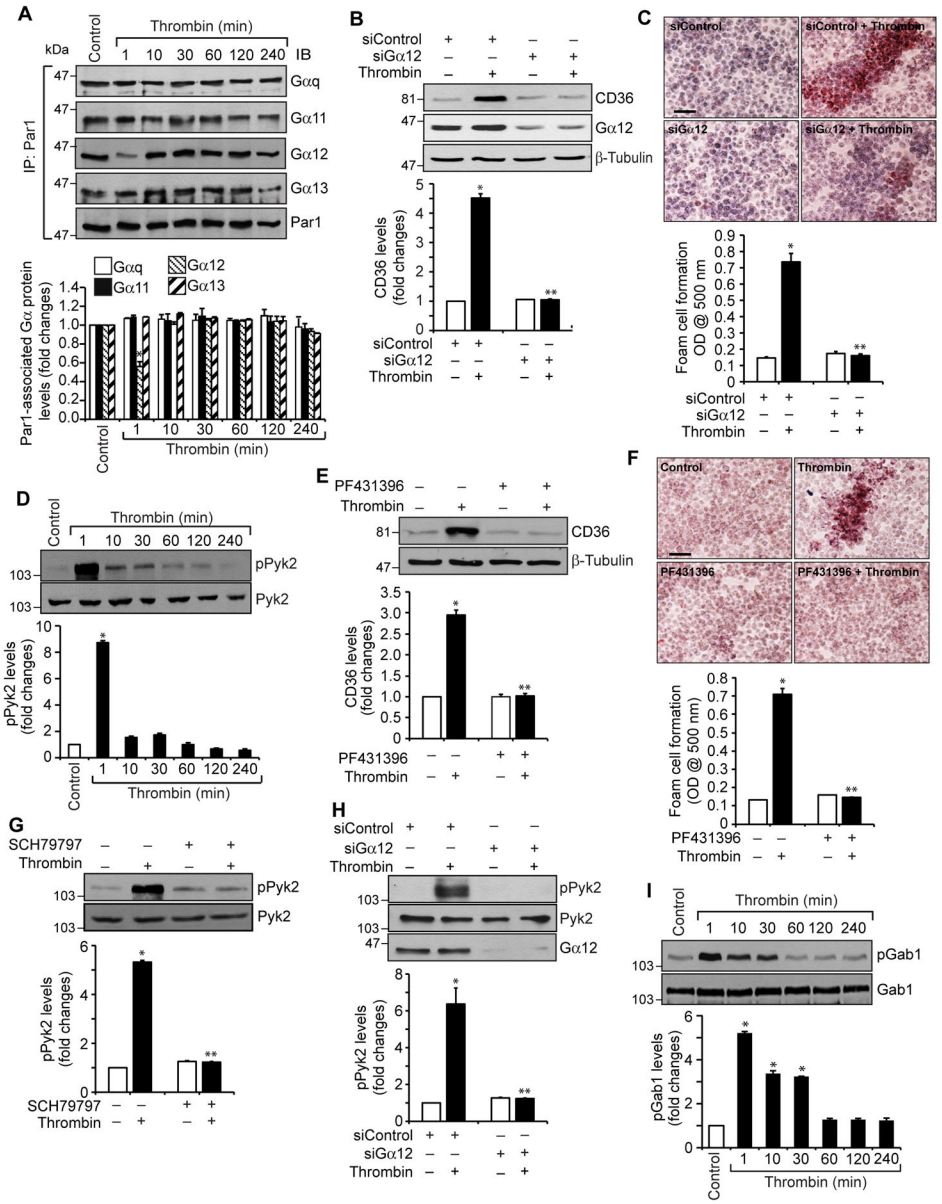

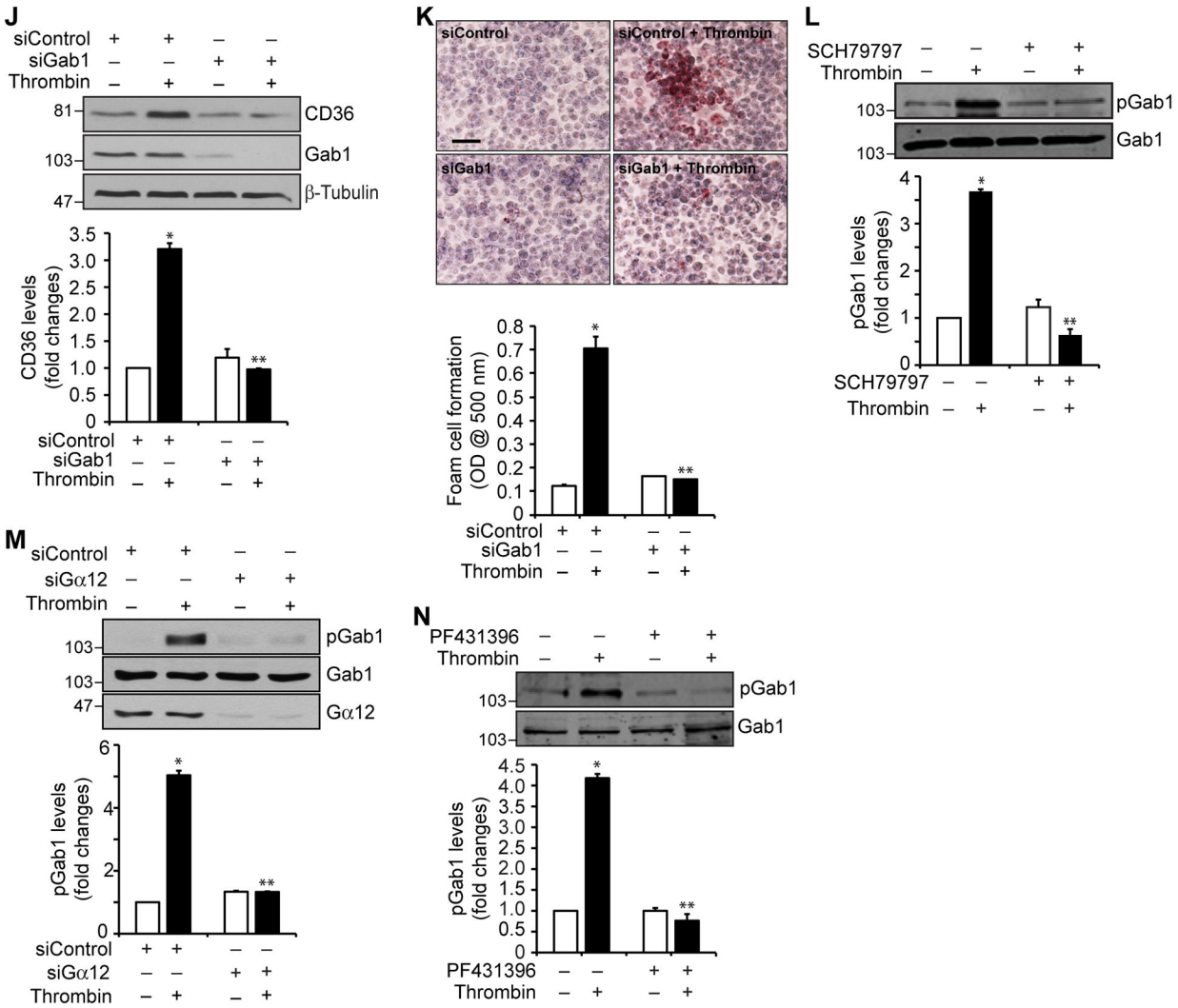

Figure 2. Gα12, Pyk2 and Gab1 mediate thrombin-induced CD36 expression and foam cell formation.

A. Equal amounts of protein from control and the indicated time periods of thrombin-treated cells were immunoprecipitated with anti-Par1 antibodies and the immunocomplexes were analyzed by Western blotting for Gαq, Gα11, Gα12 or Gα13 levels and the blot was normalized to Par1. B. Cells were transfected with siControl or siGα12 (100 nM), quiesced, treated with and without thrombin for 1 hr and analyzed by Western blotting for CD36 levels and the blot was reprobed for Gα12 or β-tubulin levels to show the effect of the siRNA on its target and off target molecules levels. C. Cells were transfected with siControl or siGα12 (100 nM), quiesced, treated with and without thrombin for 4 hrs and analyzed for foam cell formation. D. Extracts of control and the indicated time periods of thrombin-treated cells were analyzed by Western blotting for pPyk2 levels and the blot was normalized to its total levels. E. Quiescent cells were treated with and without thrombin in the presence and absence of PF431396 (5 μM) for 1 hr and analyzed by Western blotting for CD36 levels and the blot was normalized to β-tubulin levels. F. Quiescent cells were treated with and without thrombin in the presence and absence of PF431396 for 4 hrs and analyzed for foam cell

formation. G. Quiescent cells were treated with and without thrombin in the presence and absence of SCH79797 (10 μM) for 1 min and analyzed by Western blotting for pPyk2 levels and the blot was normalized to its total levels. H. All the conditions were same as in Panel B except that after quiescence the cells were treated with and without thrombin for 1 min and analyzed by Western blotting for pPyk2 levels and the blot was reprobed for Pyk2 or Gα12 levels to show the effect of the siRNA on its target and off target molecules levels. I. Extracts of control and the indicated time periods of thrombin-treated cells were analyzed by Western blotting for pGab1 levels and the blot was normalized to its total levels. J & K. Cells were transfected with siControl or siGab1 (100 nM), quiesced, treated with and without thrombin for 1 hr or 4 hrs and analyzed for CD36 levels and foam cell formation, respectively. The CD36 blot was reprobed for Gab1 or β-tubulin levels to show the effect of the siRNA on its target and off target molecules levels. L. Quiescent cells were treated with and without thrombin in the presence and absence of SCH79797 (10 μM) for 1 min and analyzed by Western blotting for pGab1 levels and the blot was normalized to its total levels. M. Cells were transfected with siControl or siGα12 (100 nM), quiesced, treated with and without thrombin for 1 min and analyzed for pGab1 levels and the blot was reprobed for Gab1 or Gα12 levels to show the effect of the siRNA on its target and off target molecules levels. N. Quiescent cells were treated with and without thrombin in the presence and absence of PF431396 (5 μM) for 1 min and analyzed for pGab1 levels and the blot was normalized for its total levels. The bar graphs represent Mean ± S.D. values of three experiments. *, $p < 0.05$ vs control or siControl; **, $p < 0.05$ vs Thrombin or siControl + Thrombin. Scale bar is 50 μm.

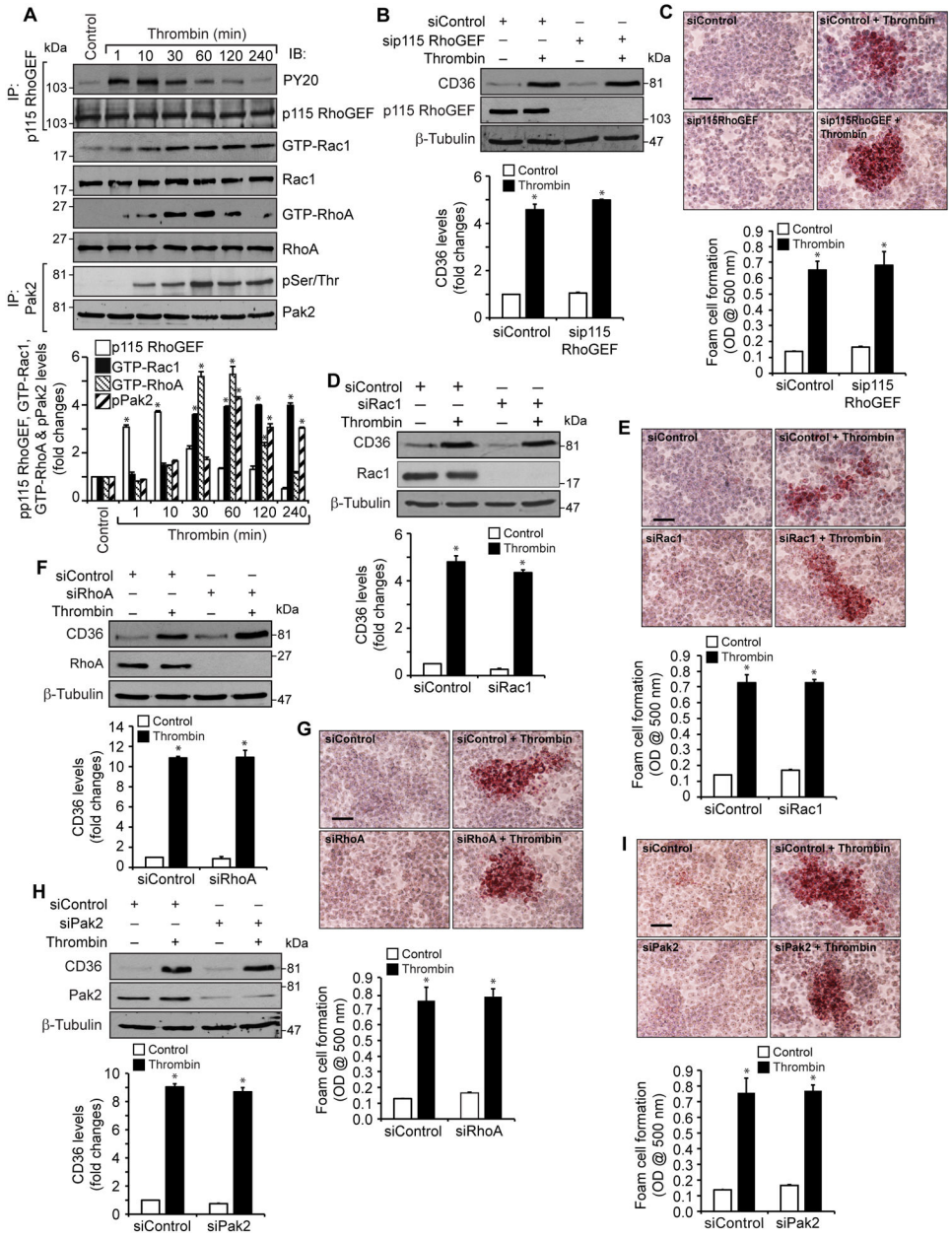

Figure 3. Lack of a role of p115 RhoGEF, Rac1, RhoA and Pak2 in thrombin- induced CD36 expression and foam cell formation.

A. Equal amounts of protein from control and the indicated time periods of thrombin-treated cells were immunoprecipitated with anti-p115 RhoGEF or anti-Pak2 antibodies and immunocomplexes were analyzed by Western blotting using anti-PY20 or anti-pSer/Thr antibodies, respectively. For GTP-Rac1 or GTP-RhoA levels, equal amounts of protein from control and the indicated time periods of thrombin- treated cells were incubated with GST-Pak1 or GST-Rhotekin-conjugated glutathione sepharose 4B beads and the pull down proteins were analyzed by Western blotting for Rac1 and RhoA levels, respectively. The same cell extracts were also analyzed by Western blotting for total Rac1 and RhoA levels. B & C. Cells were transfected with siControl or sip115 RhoGEF(100 nM), quiesced, treated

with and without thrombin for 1 hr or 4 hrs and analyzed for CD36 expression and foam cell formation, respectively. The CD36 blot was reprobed for p115 RhoGEF or β-tubulin levels to show the effect of the siRNA on its target and off target molecules levels. D & E. Cells were transfected with siControl or siRac1 (100 nM), quiesced, treated with and without thrombin for 1 hr or 4 hrs and analyzed for CD36 levels and foam cell formation, respectively. The CD36 blot was reprobed for Rac1 or β-tubulin to show the effect of the siRNA on its target and off target molecules levels. F & G. Cells were transfected with siControl or siRhoA (100 nM), quiesced, treated with and without thrombin for 1 hr or 4 hrs and analyzed for CD36 levels and foam cell formation, respectively. The CD36 blot was reprobed for RhoA or β-tubulin to show the effect of the siRNA on its target and off target molecules levels. H & I. Cells were transfected with siControl or siPak2 (100 nM), quiesced, treated with and without thrombin for 1 hr or 4 hrs and analyzed for CD36 levels and foam cell formation, respectively. The CD36 blot was reprobed for Pak2 or β-tubulin to show the effect of the siRNA on its target and off target molecules levels. The bar graphs represent Mean ± S.D. values of three experiments. *, $p < 0.05$ vs control or siControl. Scale bar is 50 μm.

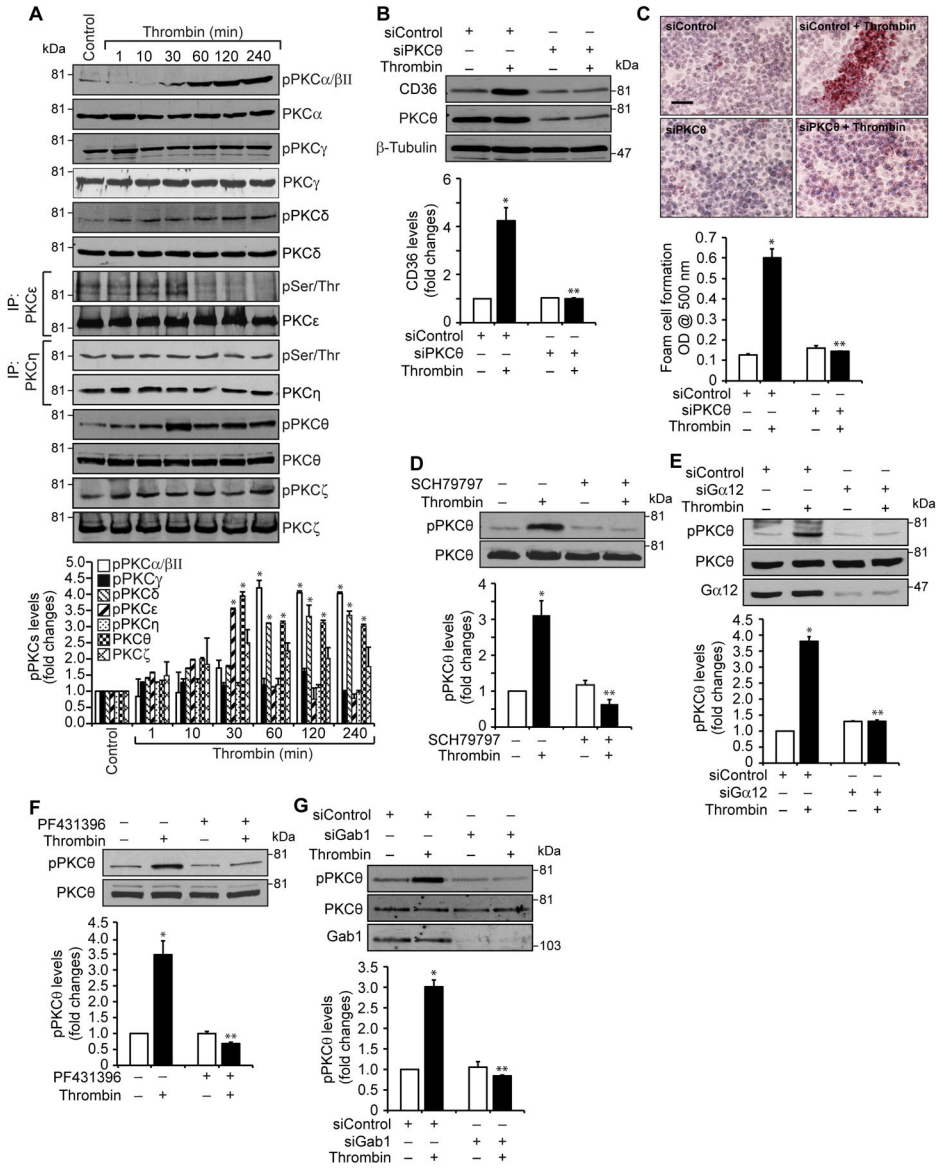

Figure 4. PKCθ mediates thrombin-induced CD36 expression and foam cell formation.

A. Equal amounts of protein from control and the indicated time periods of thrombin-treated cells were analyzed for phosphorylation of the indicated PKC isoform either by Western blotting using their phosphospecific antibodies or immunoprecipitation with pSer/Thr antibody followed by immunoblotting with the indicated PKC isoform antibody. B & C. Cells were transfected with siControl or siPKCθ siRNA, quiesced, treated with and without thrombin for 1 hr or 4 hrs and analyzed for CD36 levels and foam cell formation. The CD36 blot was reprobed for PKCθ and β-tubulin to show the effect of the siRNA on its target and off target molecules levels. D & F. Quiescent cells were treated with and without thrombin in the presence and absence of SCH79797 (10 μM) or PF431396 (5 μM) for 1 hr and analyzed by Western blotting for pPKCθ and normalized to its total levels. E & G. Cells were transfected with siControl or siGα12 siRNA, quiesced, treated with and without thrombin for 1 hr and analyzed for pPKCθ and the blots were reprobed for PKCθ, Gα12 or Gab1

levels to show the effects of the siRNAs on their target and off target molecules levels. The bar graphs represent Mean ± S.D. values of three experiments. *, $p < 0.05$ vs control or siControl; **, $p<0.05$ vs Thrombin or siControl + Thrombin. Scale bar is 50 μm.

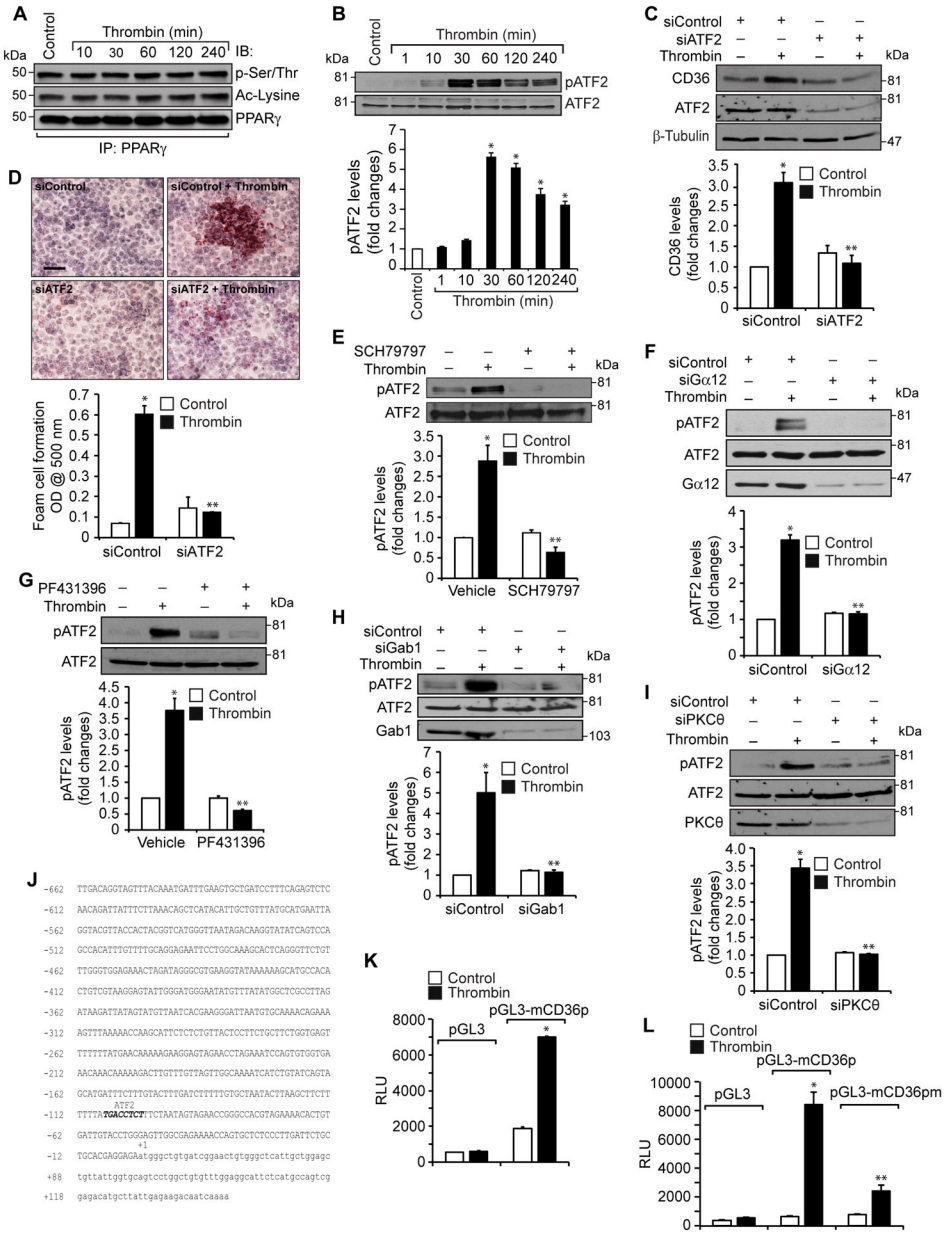

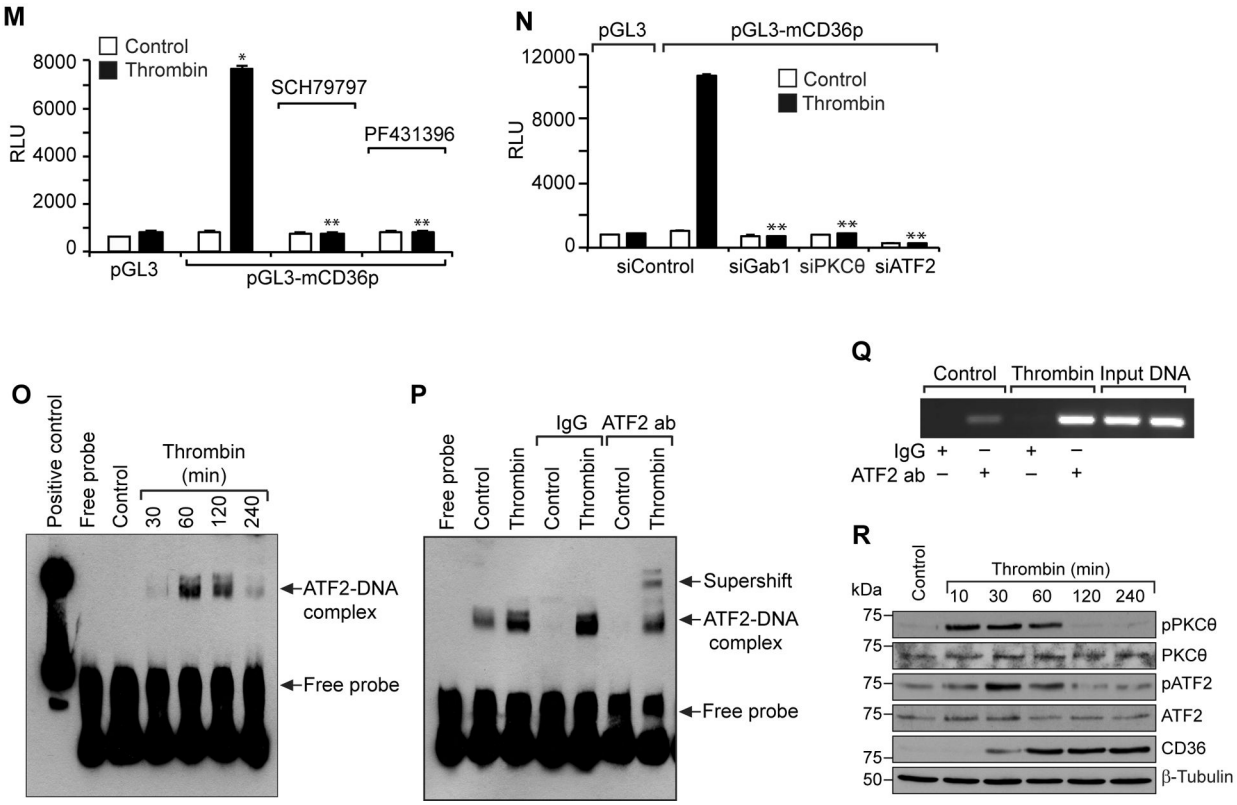

Figure 5. Par1, Gα12, Pyk2, Gab1, PKCα and ATF2 mediate thrombin-induced CD36 promoter activity.

A. Equal amounts of protein from control and the indicated time periods of thrombin-treated cells were immunoprecipitated with anti-PPARγ antibodies and the resulting immunocomplexes were analyzed by Western blotting for pSer/Thr or acetyl lysine antibodies and the blot was normalized to PPARγ levels. B. Equal amounts of protein from control and the indicated time periods of thrombin-treated cells were analyzed by Western blotting for pATF2 levels and the blot was normalized to its total levels. C & D. Cells were transfected with siControl or siATF2 (100 nM), quiesced, treated with and without thrombin for 1 hr or 4 hrs and analyzed for CD36 levels and foam cell formation. The CD36 blot was reprobed for ATF2 and β-tubulin levels to show the effect of the siRNA on its target and off target molecules levels. E & G. Quiescent cells were treated with and without thrombin in the presence and absence of SCH79797 (10 μM) or PF431396 (5 μM) for 1 hr and analyzed by Western blotting for pATF2 levels and normalized to its total levels. F, H & I. Cells were transfected with siControl, siGα12, siGab1 or siPKCθ (100 nM), quiesced, treated with and without thrombin and analyzed by Western blotting for pATF2 levels. The blots were reprobed for ATF2, Gα12, Gab1 or PKCθ to show the effects of the siRNAs on their target and off target molecules levels. J. CD36 promoter encompassing from -662 nt to +147 nt was cloned, sequenced and analyzed by TRANSFAC for transcriptional factors binding elements. K. The CD36 promoter encompassing from −662 nt to +147 nt was cloned into pGL3 vector and the RAW264.7 cells were transfected with the empty vector or pGL3-mCD36 promoter plasmids, growth-arrested, treated with and without thrombin for 6 hrs and the luciferase activity was measured. L. The RAW264.7 cells were transfected with empty

vector, pGL3-mCD36 or pGL3-mCD36m (mutant for ATF2-binding site) plasmids, growth-arrested, treated with and without thrombin for 6 hrs and the luciferase activity was measured. M. All the conditions were the same as in panel K except that after transfection and quiescence, cells were treated with and without thrombin in the presence and absence of SCH79797 (10 μM), PF431396 (5 μM) for 6 hrs and the luciferase activity was measured. N. All the conditions were the same as in panel K except that after transfection with the plasmids, cells were again transfected with siGab1, siPKCθ or siATF2 (100 nM), quiesced, treated with and without thrombin for 6 hrs and analyzed for luciferase activity. O. Nuclear extracts of control and various time periods of thrombin treated cells were analyzed by EMSA for ATF2 binding using ATF2 binding site at −107 nt as a biotin labeled oligonucleotide probe. P. Nuclear extracts of control and thrombin-treated cells were analyzed for the presence of ATF2 in the protein-DNA complexes by supershift EMSA. Q. Control and thrombin-treated cells were analyzed for ATF2 binding to CD36 promoter by ChIP assay. R. Primary peritoneal macrophages from WT mice were treated with and without thrombin for the indicated time periods and analyzed by Western blotting for pPKCθ pATF2 or CD36 levels and normalized to their total levels or β-tubulin. The bar graphs represent Mean ± S.D. values of three experiments. *, $p < 0.05$ vs control or siControl or vector; **, $p < 0.05$ vs Thrombin, siControl + Thrombin or pGL3-mCD36p + Thrombin. Scale bar is 50 μm.

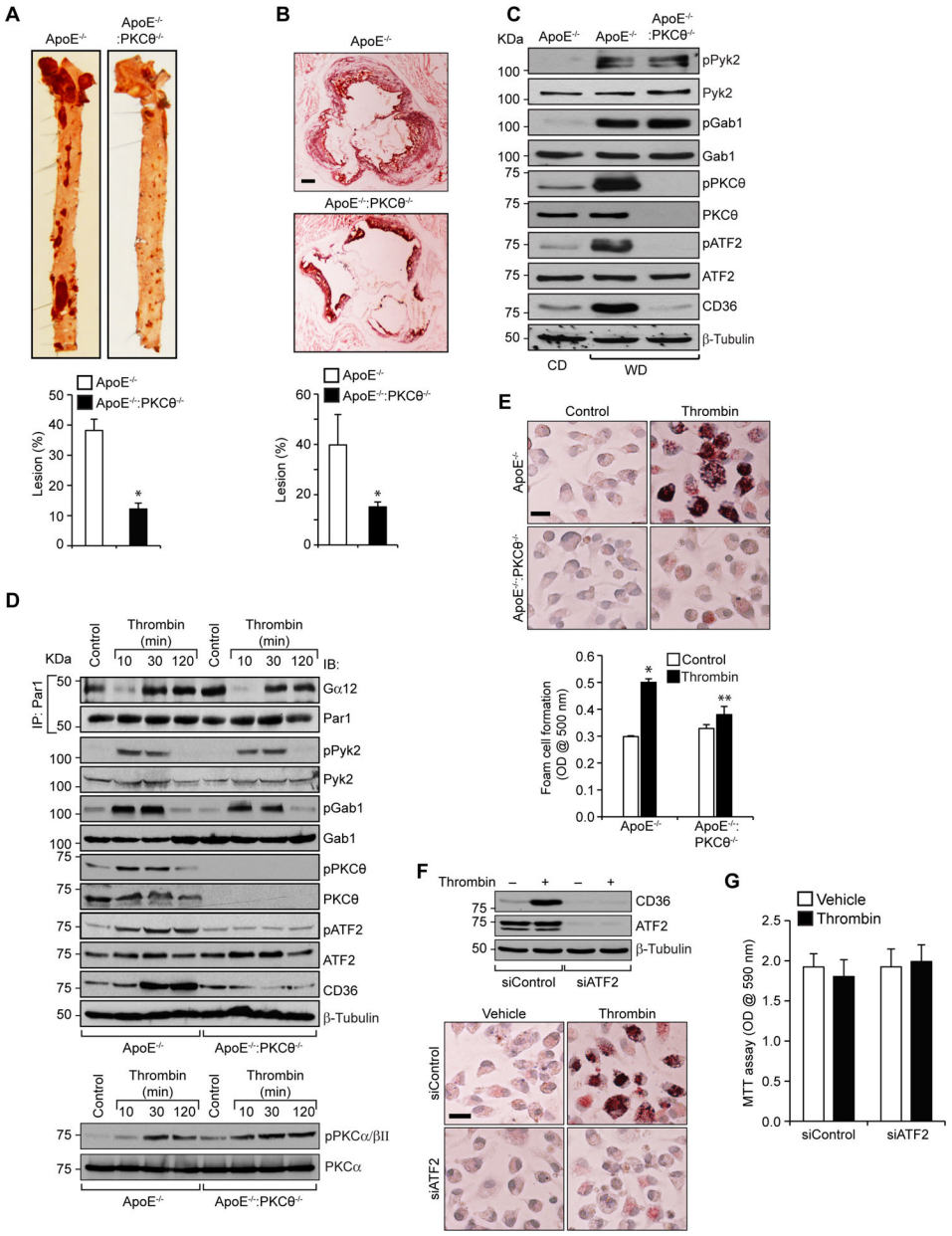

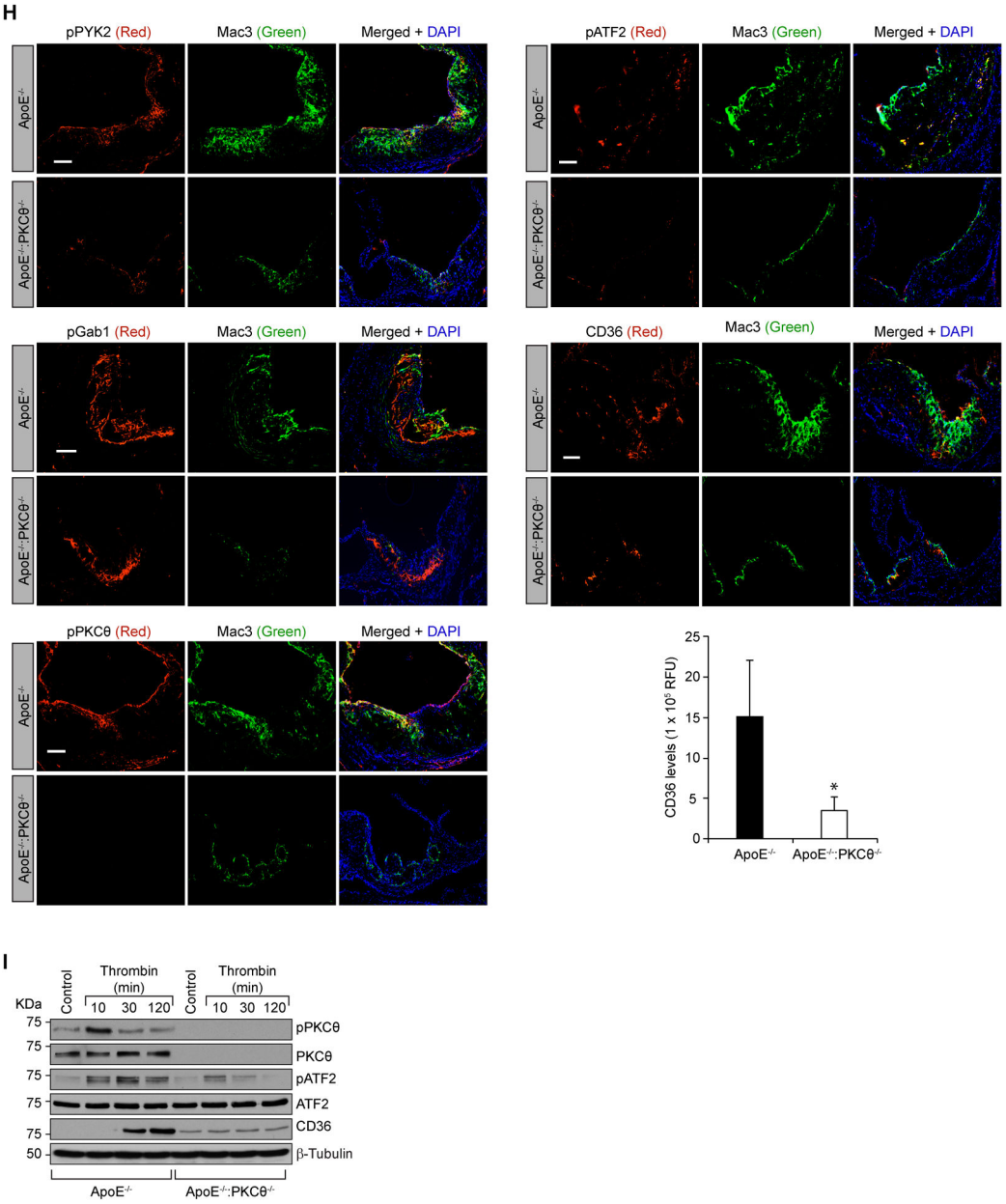

Figure 6. Genetic deletion of PKCα gene reduces the diet-induced atherosclerotic burden.

A. Representative en face staining of aortas from ApoE$^{-/-}$ and ApoE$^{-/-}$:PKCθ$^{-/-}$ mice fed with WD for 16 wks are shown and the bar graph shows the plaque area as lesion %. B. Representative Oil red O staining of the aortic root sections of the mice described in panel A are shown and the bar graph represents the quantification of the area positive for lipid staining. C. Equal amounts of protein from peritoneal macrophages of ApoE$^{-/-}$ and ApoE$^{-/-}$:PKCθ$^{-/-}$ mice fed with CD or WD for 16 wks were analyzed by Western blotting for pPyk2, pGab1, pPKCθ, pATF2 and CD36 levels and the blots were normalized to their total levels. The CD36 blot was normalized to β-tubulin. D. The peritoneal macrophages isolated from ApoE$^{-/-}$ and ApoE$^{-/-}$:PKCθ$^{-/-}$ mice were treated with and without thrombin for the indicated time periods and analyzed by Western blotting for pPyk2, pGab1, pPKCθ,

pPKCα/βII, pATF2 and CD36 levels and the blots were normalized to their total levels. The CD36 blot was normalized to β-tubulin. For Gα12 activation, the cell extracts were immunoprecipitated with anti-Par1 antibodies and the immunocomplexes were analyzed by Western blotting for Gα12 levels and the blot was normalized to Par1 levels. E. The macrophages from ApoE$^{-/-}$ and ApoE$^{-/-}$:PKCθ$^{-/-}$ mice were also analyzed for thrombin-induced foam cell formation. F & G. Peritoneal macrophages from ApoE$^{-/-}$ mice were transfected with siControl or siATF2 (100 nm), quiesced, treated with and without thrombin for 1 hr, 4 hr or 24 hr and analyzed for CD36 expression, foam cell formation and proliferation, respectively. H. The aortic root cryosections of the mice described in panel B were analyzed by double immunofluorescence staining for pPyk2, pGab1, pPKCθ, pATF2 or CD36 in combination with Mac3. I. Aortic SMCs from ApoE$^{-/-}$ and ApoE$^{-/-}$:PKCθ$^{-/-}$ mice were treated with and without thrombin for the indicated time periods and analyzed by Western blotting for pPKCθ pATF2 or CD36 levels and normalized to their total levels or β-tubulin. The bar graphs represent Mean ± S.D. values of three experiments or 7 animals. *, $p < 0.05$ vs ApoE$^{-/-}$, or control; **, $p < 0.05$ vs ApoE$^{-/-}$ + Thrombin. Scale bars are 200 μm (panel B), 20 μm (panels E & F) and 100 μm (panel H).

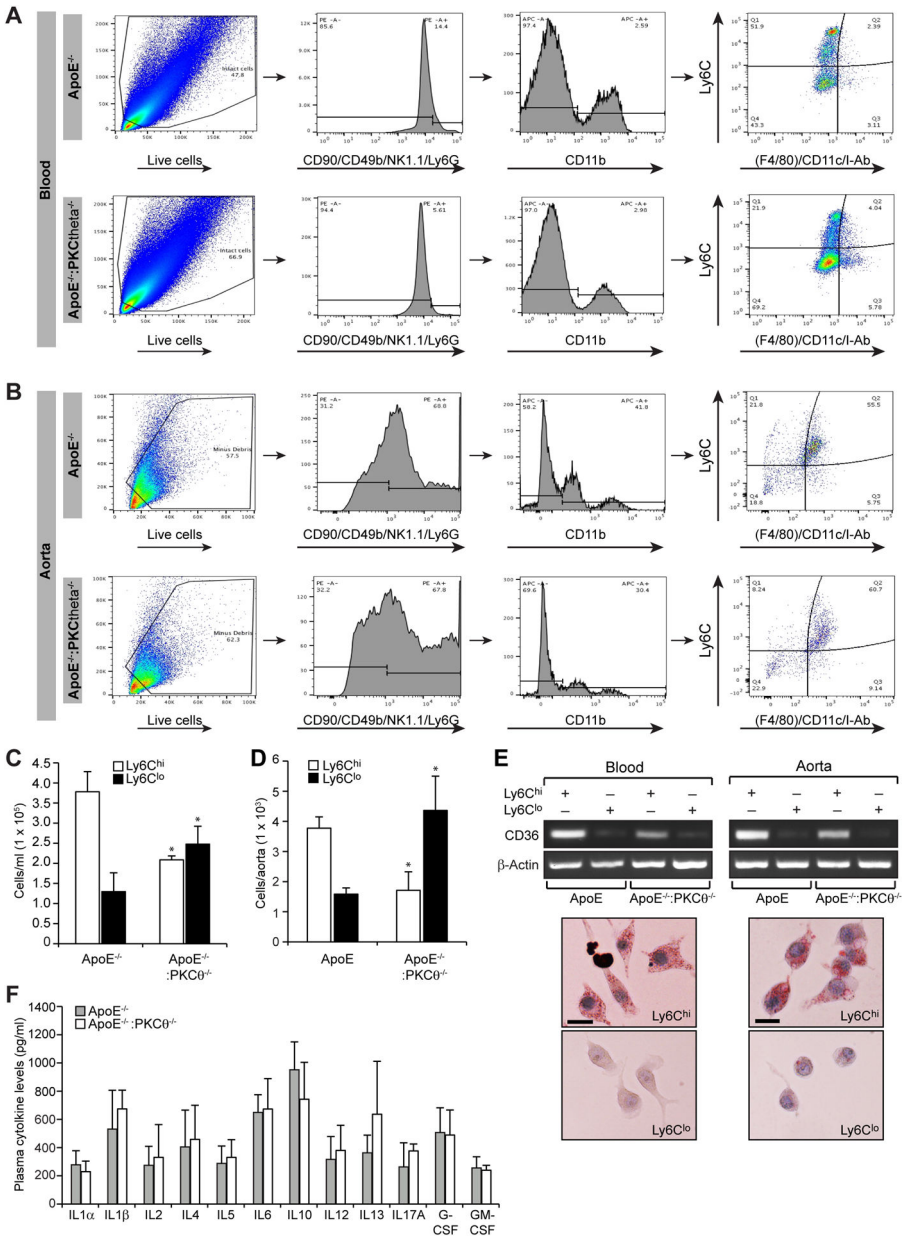

Figure 7. PKCθmediates diet-induced monocyte differentiation towards Ly6C^{hi} phenotype in ApoE$^{-/-}$ mice.

A. Blood was collected from ApoE$^{-/-}$ and ApoE$^{-/-}$:PKCθ$^{-/-}$ mice fed with WD for 16 wks, peripheral blood mononuclear cells were collected by density-gradient centrifugation, washed with RBC lysis buffer, resuspended into FACS buffer, blocked with mouse serum, washed with FACS buffer and incubated with fixable viability stain 450, anti-CD90-PE, anti-CD45R(B220)-PE, anti-CD49b-PE, anti-NK1.1-PE, anti-Ly6G-PE, anti-CD11b-APC, anti-Ly6C-FITC, anti-F4/80-PerCP-Cy5.5, anti-I-Ab-PerCP-Cy5.5 and anti-CD11c-PerCP-Cy5.5 antibodies. After washings, the cells were resuspended into sorting buffer and subjected to FACS analysis. The gating strategy is indicated as follows. Live cells (selected based on viability stain and higher forward scatter and lower side scatter) were gated as PE^{-} cells (in gate I). CD11b monocytes were gated as APC^{+} cells from PE^{-} cells (in gate II). CD11b^{+}

monocytes were gated as Ly6C^{hi}F4/80^{lo}CD11c^{lo}I-Ab^{lo}, Ly6C^{hi}F4/80^{hi}CD11c^{hi}I-Ab^{hi}, Ly6C^{lo}F4/80^{hi}CD11c^{hi}I-Ab^{hi} and Ly6C^{lo}F4/80^{lo}CD11c^{lo}I-Ab^{lo}. All gates were set using full-minus-one (FMO) controls. The percentages of each CD11b^{+} monocyte subpopulations for all mice are indicated in the respective gate. B. Aortas from ApoE$^{-/-}$ and ApoE$^{-/-}$:PKCθ$^{-/-}$ mice fed with WD for 16 wks were collected, digested with a mixture of collagenase I, collagenase XI, Dnase I and hyaluronidase, washed with Hank's balanced salt solution, resuspended in FACS buffer and subjected to FACS analysis as described in panel A. The percentages of each CD11b^{+} monocyte subpopulations for all mice are indicated in the respective gate. C & D. The bar graphs represent the number of retrieved Ly6C^{hi} and Ly6C^{lo} cells in the blood and aorta of WD-fed ApoE$^{-/-}$ mice versus ApoE$^{-/-}$:PKCθ$^{-/-}$ mice. E. The Ly6C^{hi} and Ly6C^{lo} cells were retrieved and analyzed for CD36 mRNA levels by RT-PCR or subjected to foam cell formation. F. Plasma from WD-fed ApoE$^{-/-}$ and ApoE$^{-/-}$:PKCθ$^{-/-}$ mice were analyzed for cytokines levels using mouse Multi-Analyte ELISArray Kit. Data were presented as Mean ± S.D. values of three experiments *, $p < 0.01$ vs ApoE$^{-/-}$ mice (n = 6 with 3 mice per group per experiment). Scale bar is 20 μm.

Table 1.

Plasma lipid profiles of CD and WD-fed ApoE$^{-/-}$ and ApoE$^{-/-}$:PKCθ$^{-/-}$mice.

Genotype	Diet	Weight (gm)	Cholesterol mg/dl	HDL mg/dl	LDL mg/dl	Triglycerides mg/dl	n
ApoE$^{-/-}$	CD	24.6 ± 2	340 ± 45	206 ± 23	108 ± 22	136 ± 50	6
ApoE$^{-/-}$:PKCθ$^{-/-}$	CD	23.7 ± 2	385 ± 100	214 ± 45	149 ± 59	78 ± 21 *	6
ApoE$^{-/-}$	WD	33.4 ± 3	853 ± 216	528 ± 106	283 ± 138	194 ± 59	8
ApoE$^{-/-}$:PKCθ$^{-/-}$	WD	32.3 ± 3	760 ± 271	440 ± 236	301 ± 242	138 ± 30 *	7

CD, chow diet; WD, western diet; HDL, high-density lipoprotein; LDL, low-density lipoprotein.

*, $p < 0.05$ vs ApoE$^{-/-}$ mice.